ACS APPLIED MATERIALS & INTERFACES

Research Article

www.acsami.org

Enhanced CO_2 Permeability of Membranes by Incorporating Polyzwitterion@CNT Composite Particles into Polyimide Matrix

Ye Liu,[†,‡] Dongdong Peng,[†,‡] Guangwei He,[†,‡] Shaofei Wang,[†,‡] Yifan Li,[†,‡] Hong Wu,[†,‡] and Zhongyi Jiang*[,†,‡]

[†]Collaborative Innovation Center of Chemical Science and Engineering (Tianjin), Tianjin 300072, China

[‡]Key Laboratory for Green Chemical Technology of Ministry of Education, School of Chemical Engineering and Technology, Tianjin University, Tianjin 300072, China

ABSTRACT: In this study, polyzwitterion is introduced into a CO_2 separation membrane. Composite particles of polyzwitterion coated carbon nanotubes (SBMA@CNT) are prepared via a precipitation polymerization method. Hybrid membranes are fabricated by incorporating SBMA@CNT in polyimide matrix and utilized for CO_2 separation. The prepared composite particles and hybrid membranes are characterized by transmission electron microscopy (TEM) with element mapping, field emission scanning electron microscopy (FESEM), Fourier transform infrared (FTIR) spectra, differential scanning calorimetry (DSC) and an electronic tensile machine. Water uptake and water state of membranes are measured to probe the relationship among water uptake, water state and CO_2 transport behavior. Hybrid membranes show significantly enhanced CO_2 permeability compared to an unfilled polyimide membrane at a humidified state. A hybrid membrane with 5 wt % SBMA@CNT exhibits the maximum CO_2 permeability of 103 Barrer with a CO_2/CH_4 selectivity of 36. The increase of CO_2 permeability is attributed to the incorporation of the SBMA@CNT composite particles. First, SBMA@CNT form interconnected channels for CO_2 transport due to the facilitated transport effect of the quaternary ammonium in repeat unit of pSBMA. Second, SBMA@CNT improve water uptake and adjust water state of membrane, which further increases CO_2 permeability. Meanwhile, the variation of CO_2/CH_4 selectivity is dependent on the bound water portion in the membrane. A gas permeation test at a dry state and a pressure test are conducted to further probe the membrane separation performance.

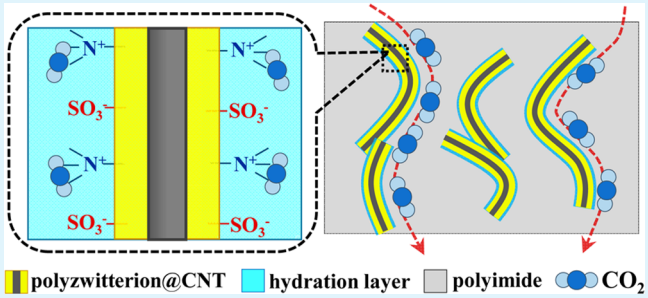

KEYWORDS: *polyzwitterion, polyimide, hybrid membrane, quaternary ammonium, water, CO_2 separation*

1. INTRODUCTION

CO_2 capture is a crucial industrial process due to the necessity of natural gas purification and the urgency of controlling global warming.[1−3] Polymer-based membrane gas separation is considered as a promising technology for CO_2 capture because of the prominent advantages of high energy efficiency, design flexibility, scale-up simplicity and environmental friendliness.[4−6] Generally, a good gas separation membrane should possess high permeability, desirable selectivity, robust mechanical property and good operation stability.[7,8] Nowadays, glassy polymers constitute the majority of membrane materials, attributed to their high separation factor.[9−12] The compact chain packing below glass transition temperature endows glassy polymers with desirable diffusion selectivity for gas separation as well as good mechanical and thermal stability.[13,14] However, the gas transport property in a glassy polymer membrane is quite sensitive to the inherent structure of a polymer,[15] i.e., interchain spacing and chain mobility. Thus, a glassy polymer membrane with high selectivity often has relatively low permeability,[7,16,17] which should be rationally solved for practical application.

Polyimide is a most representative type of glassy polymer and is widely considered as the preferred membrane material for CO_2 capture.[18−24] A lot of studies focus on increasing the CO_2 permeability of polyimide membranes. An effective approach is the specific tailoring of the polyimide molecular structure by incorporating bulky bridging groups via chemical synthesis, which could restrain polymer chain packing, increase fractional free volume of membrane, thereby increasing CO_2 permeability.[25−27] Another simple and versatile approach is to prepare a hybrid polyimide membrane by incorporating selective or nonselective particles,[28−36] which are expected to adjust polymer chain mobility, affect interfacial morphology, construct gas diffusion routes or facilitate CO_2 transport, ultimately increasing CO_2 permeability. However, in consideration of the industrial demand of CO_2 permeance, further efforts are still needed to fabricate a highly permeable polyimide membrane with desirable selectivity. It is another noticeable problem that few polyimide membranes perform well at a humidified state in

Received: May 13, 2014
Accepted: July 28, 2014
Published: July 28, 2014

Scheme 1. Preparation Process of the SBMA@CNT Composite Particles

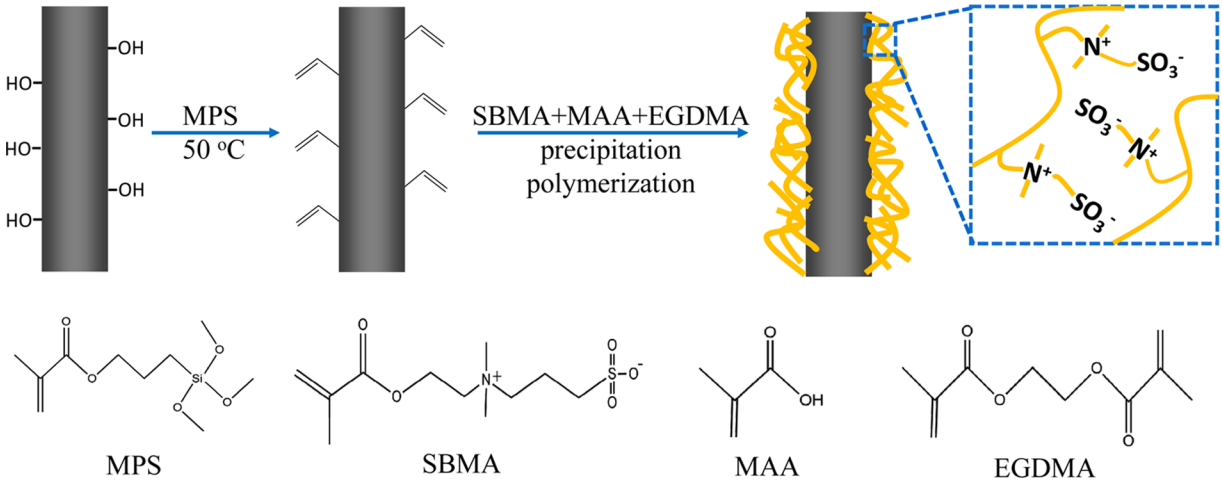

reported studies because the polymer chain of polyimide is highly hydrophobic and rigid. A highly hydrophobic polymer chain could not absorb sufficient water to benefit from water swelling, whereas a rigid polymer chain would even suffer from a blockage effect or the competitive adsorption between water and CO_2 molecules.[37−40] Considering that water is an essential component in feed gases of CO_2 separation,[41,42] it is necessary to exploit novel methods to improve the performance of a hydrophobic polymer membrane at a humidified state.

Very recently, polyzwitterion has attracted much attention in the research of biomedical and engineering materials because of its super hydrophilic property.[43−45] Owing to the unique structure, polyzwitterion could bind water via electrostatic interaction while other hydrophilic materials, e.g., poly(ethylene glycol), form the hydration via hydrogen bond interaction.[46] Research of poly(sulfobetaine methacrylate) (pSBMA), a typical polyzwitterion, indicates that eight water molecules could be strongly bonded on each sulfobetaine unit while more water molecules are loosely adsorbed simultaneously.[47,48] Besides the strong water hydration capacity, pSBMA might have preferential affinity toward CO_2 because the quaternary ammonium in its repeat unit is considered to be able to facilitate CO_2 transport.[49,50] However, to the best of our knowledge, few studies utilize polyzwitterion in preparing CO_2 separation membranes.

In this study, we attempt to incorporate polyzwitterion in polymeric membrane to enhance CO_2 separation performance. A hybrid membrane is designed by filling polyzwitterion@CNT composite particles into a polyimide matrix. Specifically, pSBMA is selected as a multifunctional additive to effectively increase CO_2 permeability. The carbon nanotube (CNT) is selected as the supporter for pSBMA because it is unique in shape and easily modified. Polyimide is selected as the polymer matrix because it is a typical glassy polymer with a rigid and hydrophobic chain. The interconnected SBMA@CNT composite particles are prepared and used to fabricate a hybrid membrane. The hybrid membranes show significantly enhanced CO_2 permeability and desired selectivity at a humidified state. Water uptake and water state of membranes are measured to probe the relationship among water uptake, water state and CO_2 transport behavior.

2. EXPERIMENTAL SECTION

2.1. Materials. Matrimid 5218 (PI), 3-(methacryloxy) propyltrimethoxysilane (MPS) and ethylene glycol dimethacrylate (EGDMA) were purchased from Alfa Aesar China Co., Ltd. Hydroxyl modified multiwalled carbon nanotubes (CNT) were purchased from Nanjing XFNANO Materials Tech Co., Ltd. Zwitterionic monomer, *N*-(3-sulfopropyl)-*N*-(methacryloxyethyl)-*N*,*N*-dimethylammonium betaine (SBMA) was purchased from Sigma-Aldrich. Methacrylic acid (MAA), 2,2′-azoisobutyronitrile (AIBN), *N*,*N*-dimethylformamide (DMF) and ethanol were purchased from Tianjin Guangfu Fine Chemical Engineering Institute. Acetonitrile was purchased from Tianjin Kewei Co., Ltd. Deionized water was used in the whole experiment.

2.2. Preparation of the SBMA@CNT Composite Particles. As shown in Scheme 1, CNT and MPS were first blended in ethanol and reacted at 50 °C for 48 h to graft CNT with C═C bonds. Then the polymerization of SBMA on the modified CNT was conducted through precipitation polymerization method.[51,52] The specific procedure was as follows: 0.04 g of aforementioned modified CNT was dispersed in a mixture of acetonitrile−water (3:1 vol %) assisted by ultrasonication for 1 h. Afterward, 0.4 g of SBMA, 0.02 g of AIBN, 0.1 mL of MAA and 0.4 mL of EGDMA were added in the mixture at 25 °C. Then the mixture was heated to boiling state and reacted for 80 min. After separated and washed with ethanol, the products were dried at 40 °C in a vacuum oven for 24 h.

2.3. Preparation of the Membrane. Unfilled PI membrane was prepared by casting a 6 wt % PI solution (DMF as solvent) onto a glass mold. The solvent evaporation process was conducted at 50 °C for 12 h. Then the membrane was treated for 12 h at 80 °C and another 48 h at 120 °C. As for the preparation of hybrid membranes, a certain amount of SBMA@CNT composite particles was added in DMF solvent and dispersed for 10 min by an ultrasonic cell disruption machine, then further dispersed by an ultrasonic machine for 1 h. Afterward, PI was added into the suspension and stirred for 5 h to obtain a 6 wt % PI solution with dispersed SBMA@CNT composite particles. The membrane casting procedure and post processing were similar to the unfilled PI membrane. Hybrid membranes were denoted as PI-SBMA@CNT(x), where x is the particle content (wt %) in polymer matrix.

2.4. Characterization and Water Measurement. Morphology and elemental mapping of the composite particles were obtained by a transmission electron microscopy (TEM, Tecnai G2 20 S-TWIN). Cross section morphology of membrane was observed with field emission scanning electron microscopy (FESEM, Hitachi S-4800). Fourier transform infrared (FTIR) spectra of the particles and membranes were obtained with a FTIR spectrometer (Nicolet FTIR 6700 equipped with horizontal attenuated total reflectance accessory). Glass transition temperatures of membranes were measured with a

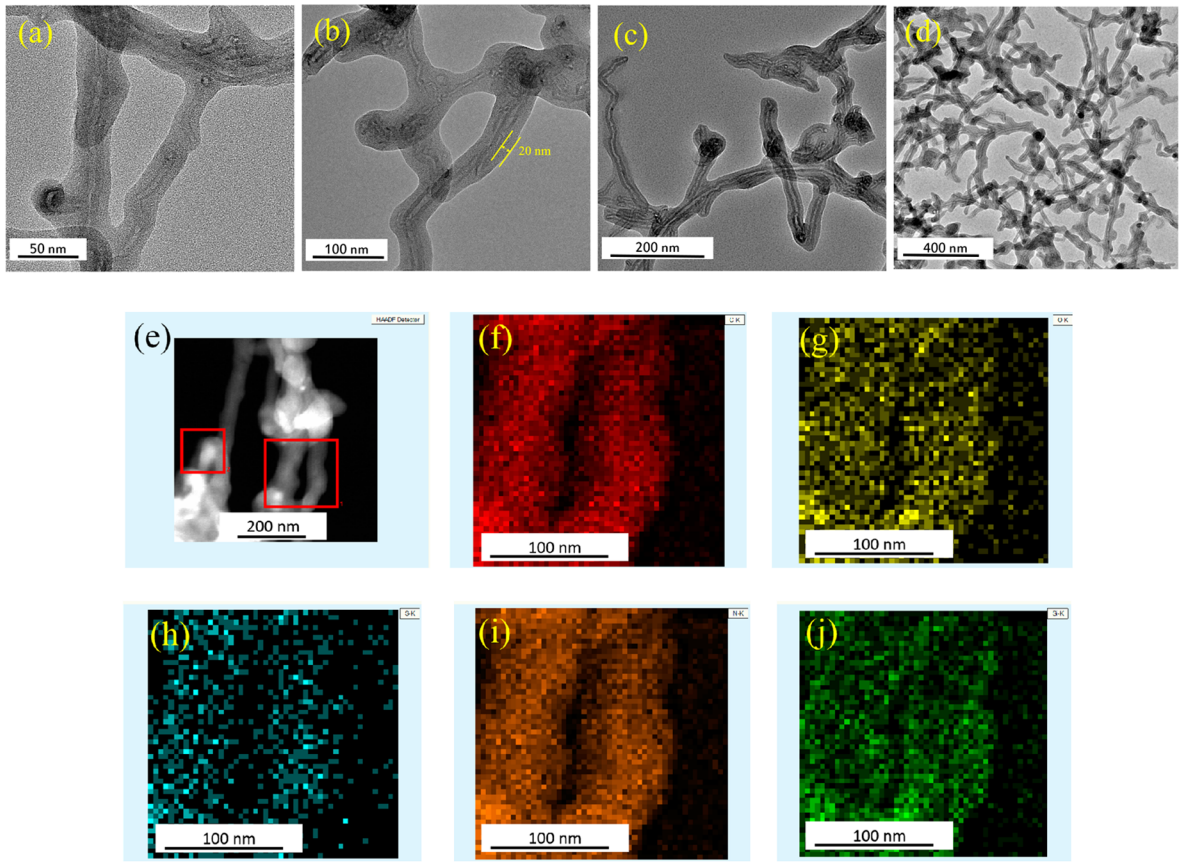

Figure 1. TEM images and element mapping of SBMA@CNT composite particles.

Netzsch DSC 200F3 calorimeter in the temperature range of 50−400 °C. Mechanical properties of membranes were measured by an electronic tensile machine (Yangzhou Zhongke WDW-02).

Water uptake and water state in membranes were measured with the method described in literature.[53] Membranes were weighed (m_1) after gas permeation experiments. Then the membranes were heated at 100 °C for 12 h in an oven to remove free water and reweighed (m_2). Afterward, the membranes were heated again at 150 °C for 12 h to remove bound water then reweighed (m_3). The content of total water (W_t, %), free water (W_f, %) and bound water (W_b, %) could be calculated by eqs 1, 2 and 3, respectively.

$$W_t = (m_1 - m_3)/m_3 \times 100\% \quad (1)$$

$$W_f = (m_1 - m_2)/m_3 \times 100\% \quad (2)$$

$$W_b = (m_2 - m_3)/m_3 \times 100\% \quad (3)$$

2.5. Gas Permeation Test. A mixed gas CO_2/CH_4 (30/70 vol %) permeation test of the humidified membrane was conducted at 30 °C in a feed pressure range of 2−16 bar using a conventional constant pressure/variable volume technique. Membranes samples had been immersed in water for 10 days to get sufficient water absorption before they were tested. The test apparatus scheme was described in our previous work.[54] Typical measurement was conducted at 2 bar. Feed gas was saturated with water vapor (relative humidity >98%)[55,56] by passing through a water bottle (35 °C). N_2 was used as a sweep gas and humidified at room temperature. The composition of the permeate gas was measured every 10 min until the data was steady (at least 6 h) using gas chromatography (Agilent 6820). Gas permeability (P_i, Barrer, 1 Barrer = 10^{-10} cm^3 (STP) cm/(cm^2 s cmHg)) was obtained from average value of two tests by eq 4.

$$P_i = \frac{Q_i l}{\Delta p_i A} \quad (4)$$

where Q_i is the gas volumetric flow rate (cm^3/s)(STP), l is the membrane thickness (cm), Δp_i is partial pressure difference across the membrane (cmHg) and A is the effective membrane area (cm^2). The mixed gas selectivity (α_{ij}) was calculated by eq 5.

$$\alpha_{ij} = \frac{P_i}{P_j} \quad (5)$$

Gas permeability of dry membrane was also tested for comparison and assistant elucidation. Because the gas permeability of a Matrimid membrane at a dry state was minor compared with a humidified state, it was tested by "time-lag" method[57] to get accurate result. To be comparable with the aforementioned humidified test, dry membrane samples had been kept at 40 °C for 10 days after they were prepared and then used for the gas permeation test. The test was conducted at 30 °C and 2 bar of the high-pressure side after being evacuated for 8 h to remove the possibly dissolved species in membranes.

3. RESULTS AND DISCUSSION

3.1. Characterization. The morphology and element mapping of SBMA@CNT composite particles are obtained by transmission electron microscopy (TEM). As shown in Figure 1a−d, the pSBMA layer (about 20 nm) is coated on CNT through a precipitation polymerization method. The particles show an interconnected channel morphology without obvious aggregation. Element mapping of the region in the right square in Figure 1e is shown in Figure 1f−j, for C, O, S, N and Si, respectively. S and N are characteristic elements of pSBMA whereas Si is a characteristic element of the cross-link agent in the synthetic process of particles. Elements mapping confirms that the pSBMA layer is coated on CNT and well-distributed.

The morphology of membrane cross section is observed with field emission scanning electron microscopy (FESEM). As shown in Figure 2, membrane structures are strongly affected

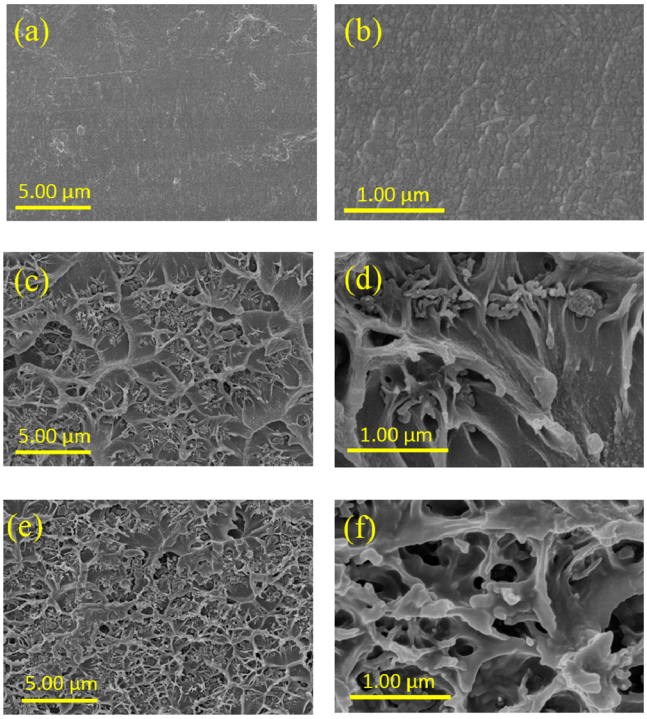

Figure 2. SEM images of cross section of membranes (a, b) unfilled PI membrane, (c, d) PI-SBMA@CNT(2) and (e, f) PI-SBMA@CNT(10).

by the incorporation of particles. Hybrid membranes show rougher cross sections than that of unfilled PI membrane. Meanwhile, the incorporation of particles forms interconnected network morphology and high particle loading generates defects in membrane. Besides, SBMA@CNT composite particles are dispersed in the polymer matrix without severe aggregation, resulting in a relatively uniform cross section morphology.

Chemical structures of the particles and membranes are confirmed by FTIR spectra. As shown in Figure 3a, spectrum of SBMA@CNT composite particles presents characteristic bands at 1720 cm^{-1} due to stretching vibration of esterified carbonyl, 1170 cm^{-1} due to organic sulfate, 1030 cm^{-1} due to quaternary ammonium, corresponding to the chemical structure of SBMA.[58] The spectrum of the unfilled PI membrane shows characteristic bands at 1780 cm^{-1} and 1720 cm^{-1} due to the stretching vibration of C═O bond in imide ring and at 1360 cm^{-1} due to stretching vibration of C−N bond in the imide ring, corresponding to the chemical structure of PI.[59] Hybrid membranes show similar characteristic spectra to the unfilled PI membrane without distinct variation. However, because both SBMA@CNT and polyimide show characteristic bands at 1720 cm^{-1}, spectra of hybrid membranes with high particle content show a split near 1720 cm^{-1}, which might be caused by the influence between similar band positions of groups.

Glass transition temperatures (T_g) of membranes are measured by differential scanning calorimetry (DSC). As shown in Figure 4, the T_g of unfilled PI membrane is about 328 °C whereas T_g of the hybrid membranes slightly decrease with the increment of the particle content. The PI-SBMA@

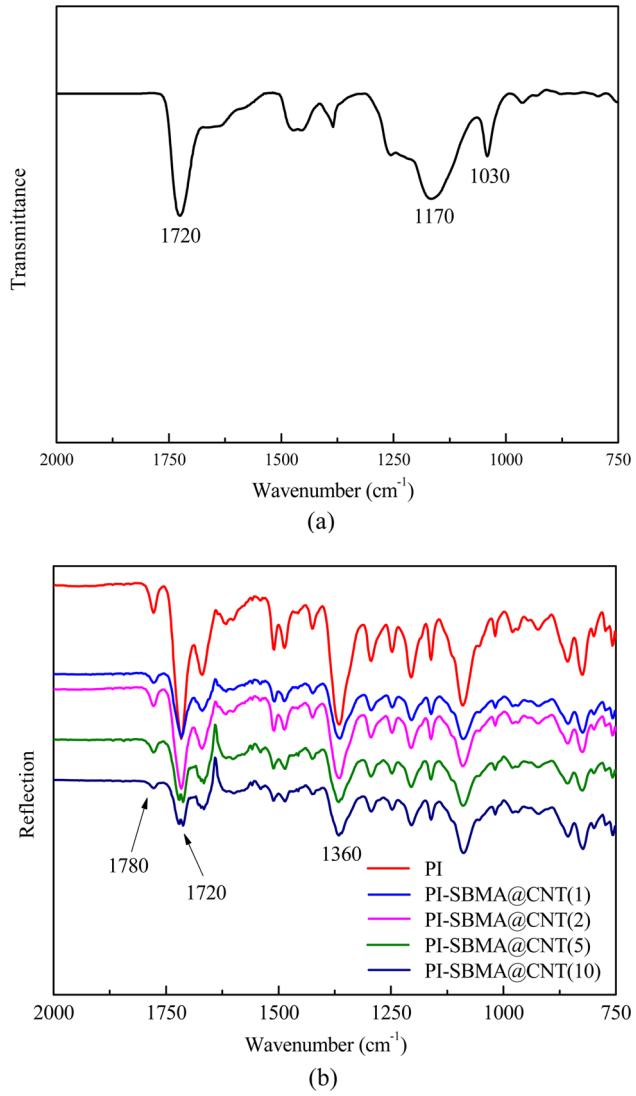

Figure 3. (a) FTIR spectrum of SBMA@CNT composite particles (b) FTIR spectra of membranes.

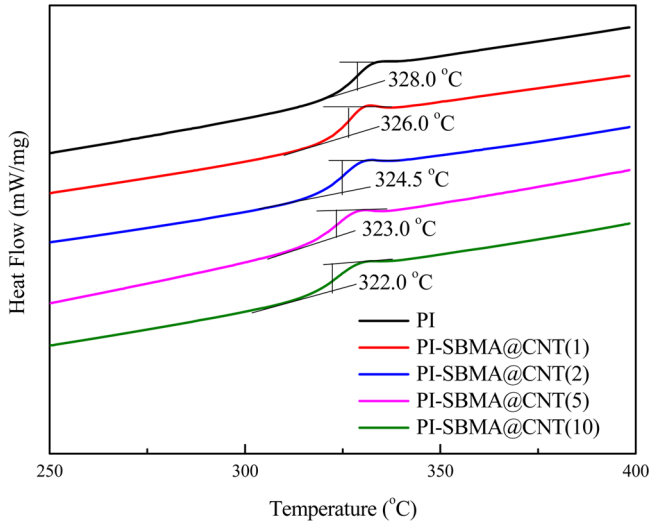

Figure 4. DSC curves of membranes.

CNT(10) membrane shows a glass transition at about 322 °C. Because T_g is commonly related to polymer chain mobility, the

dx.doi.org/10.1021/am502936x | ACS Appl. Mater. Interfaces 2014, 6, 13051−13060

variation of T_g indicates that the incorporation of particle does not cause severe rigidification of polymer chains whereas slightly enhances polymer chain mobility. The reason might be that the polyzwitterion layer weakens the rigidification effect of uncoated CNT[30,31] in polymer membrane matrix.

Mechanical properties of membranes are tested after the humidified gas permeation test (Table 1). In general, the incorporation of the particle results in a decreased strength and plasticity but an increased elasticity of the membranes. The results could be explained as follows: because incorporating interconnected particles causes defects structure such as cavity and void in membranes, the strength and plasticity of the membranes decrease with the increased particle content. However, when the particle content further increases to 10 wt %, the strength and plasticity of the membranes turn to increase due to the strong cohesion between the pSBMA layer on the particles. However, the elasticity of membranes improves with the incorporation of the particles, which might be attributed to the extreme high Young's modulus of CNT.

Table 1. Mechanical Properties of Membranes (25 °C)

membrane	break strength (MPa)	maximum elongation (%)	Young's modulus (MPa)
PI	79 ± 3	15.90 ± 0.90	1382 ± 52
PI-SBMA@CNT(1)	77 ± 3	5.91 ± 0.41	1492 ± 59
PI-SBMA@CNT(2)	74 ± 1	5.87 ± 0.16	1398 ± 33
PI-SBMA@CNT(5)	34 ± 2	1.91 ± 0.11	1759 ± 77
PI-SBMA@CNT(10)	55 ± 3	4.89 ± 0.28	1134 ± 42

3.2. Water Uptake and Water State. Because water is a major concern in this study, water uptake and water state are measured to probe the relationship between water and CO_2 transport. As shown in Table 2, water uptake of hybrid membrane is generally higher than that of unfilled PI membrane and reaches a maximum when the particle content is 5 wt %. Meanwhile, bound water portion of hybrid membrane is generally higher than that of unfilled PI membrane but reaches a minimum when the particle content is 5 wt %.

Table 2. Water Uptake and Water State

membrane	total water (g/g membrane)	bound water/ total water (%)	free water/ total water (%)
PI	0.107 ± 0.004	19.5 ± 0.9	80.5 ± 0.9
PI-SBMA@CNT(1)	0.109 ± 0.003	25.2 ± 1.1	74.5 ± 1.1
PI-SBMA@CNT(2)	0.109 ± 0.002	22.9 ± 0.6	77.1 ± 0.6
PI-SBMA@CNT(5)	0.116 ± 0.005	17.2 ± 0.7	82.8 ± 0.7
PI-SBMA@CNT(10)	0.110 ± 0.005	22.7 ± 0.9	77.3 ± 0.9

These results could be interpreted by combining the effect of pSBMA and the structure feature of hybrid membranes. When SBMA@CNT is first incorporated in membranes, water uptake of membrane increases due to the excellent hydrophilicity of pSBMA. It could tightly bind water molecules at the positively charged group ($N^+(CH_3)_3$) and the negatively charged group (SO_3^-) via electrostatic interaction,[48] forming a bound water layer at the interface between the particle and polymer matrix. Then an additional free water layer would form on the bound water layer,[60,61] which further increases the total water uptake but decreases the bound water portion. When the particle content is 5 wt %, major free water is absorbed in polymer matrix resulting in the maximum water uptake but minimum bound water portion. It is should be noticed that, when the particle content becomes even higher as 10 wt %, the total water uptake turns to decrease. It is because strong cohesion forms between the excessively interconnected structures of SBMA@CNT, confining the entire membrane structure, limiting free water further absorbed in membrane.

3.3. Gas Permeation Test. *3.3.1. Dry Gas Permeation.* Pure gas permeability at dry state is tested for comparison and assistant elucidation. As shown in Table 3, the incorporation of SBMA@CNT causes a decline of CO_2 permeability and an increase of CO_2/CH_4 selectivity of membranes. The decline of CO_2 permeability should be ascribed to the addition of the impermeable particles. Although the DSC result implies a slight improvement of polymer chain mobility with the incorporation of SBMA@CNT, the close-ended particles form an impermeable region in the polymer matrix, leading to more tortuous gas transport routes in the membrane. Besides, at the dry state, pSBMA does not show a distinct facilitated transport effect on CO_2 molecule. Thus, CO_2 permeability shows a certain decline. Meanwhile, with larger kinetic diameter, CH_4 permeability decreases more severely with the incorporation of particles, leading to an increased CO_2/CH_4 selectivity of the membrane.

Table 3. CO_2 Permeability and CO_2/CH_4 Selectivity of Membranes at Dry State

membrane	CO_2 permeability (Barrer)	CO_2/CH_4 selectivity
PI	6.2 ± 0.3	42.8 ± 2.1
PI-SBMA@CNT(1)	5.9 ± 0.2	45.2 ± 1.8
PI-SBMA@CNT(2)	5.7 ± 0.2	48.8 ± 2.4
PI-SBMA@CNT(5)	4.8 ± 0.1	73.3 ± 3.3
PI-SBMA@CNT(10)	4.1 ± 0.2	97.0 ± 4.5

3.3.2. Humidified Gas Permeation. Separation properties of membranes at a humidified state are completely different from the previously discussed dry state. As shown in Figure 5, CO_2 permeability significantly increases when incorporating SBMA@CNT in the polymer matrix. It shows a maximum increment of about 107% compared to the unfilled PI membrane when the particle content is 5 wt %. Meanwhile, the selectivity of CO_2/CH_4 first increases when the particle content is 1 wt %, then shows a decline and reaches a minimum when the particle content is 5 wt %. Comparing the difference between membrane performance at dry state and at humidified state, it could be inferred that water plays a key role in the separation process.

In the presence of water, the enhanced CO_2 permeability of membrane could be interpreted by the structure−property relationship. First, it should be attributed to the facilitated transport effect of SBMA@CNT composite particles. As we know, quaternary ammonium is considered to effectively facilitate CO_2 transport due to the specific interaction between quaternary nitrogen and CO_2 in the presence of water.[49] In this study, the pSBMA layer containing quaternary nitrogen is coated on CNT through precipitation polymerization, which provides more dense functional groups compared with other modification methods of CNT such as surface treatment, noncovalent functionalization and chemical grafting.[62−64] To detect the specific interaction between CO_2 and the hybrid membrane, we conduct FTIR measurements of CO_2 adsorption and desorption within membranes because it is commonly

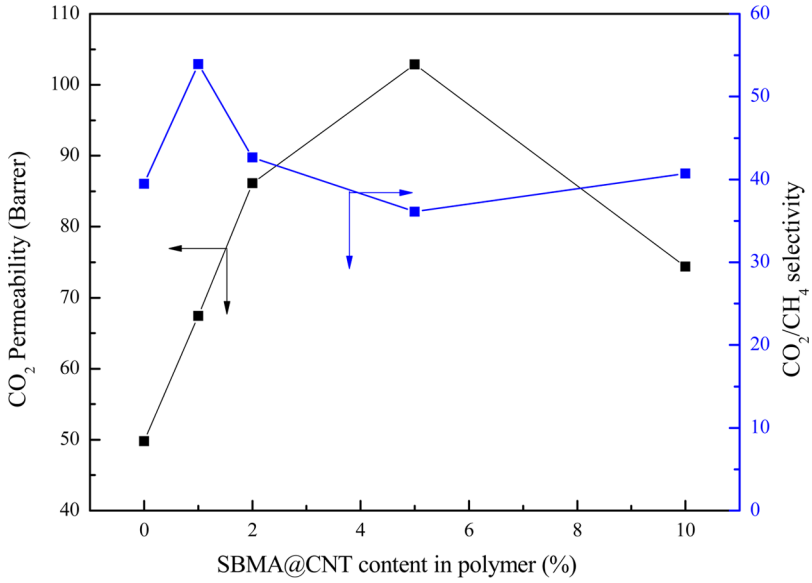

Figure 5. CO_2 permeability and CO_2/CH_4 selectivity of membranes at humidified state.

employed as a simple method to examine facilitated transport.[65,66] The unfilled PI membrane and PI-SBMA@CNT(5) membrane are used for comparison. CO_2-absorbed membrane samples were prepared by putting membranes in humidified CO_2-filled sample bags for 6 h. CO_2-desorbed membrane samples were prepared by exposing the aforementioned CO_2-absorbed membrane samples to humidified air for 6 h. As shown in Figure 6b, the CO_2-absorbed PI membrane (spectrum B) shows a new peak at 2400−2300 cm^{-1}, corresponding to the CO_2 asymmetric stretching vibration compared with the original PI membrane (spectrum A). This peak disappears after CO_2 is desorbed from the PI membrane (spectrum C), confirming that the peak arises from the absorption of CO_2. The CO_2-absorbed hybrid membrane (spectrum E) shows some new peaks in the regions marked in Figure 6 (a) compared with the original hybrid membrane (spectrum D), indicating that new bonds form when hybrid membrane absorbs CO_2.[65] Some of the new peaks are hard to identify whereas the peaks assigned to CO_2 are distinct, confirming the reversible interaction. The peak at 2345 cm^{-1} corresponding to CO_2 asymmetric stretching vibration appears to be more sharp and strong but less broad than CO_2-absorbed PI membrane (spectrum B), which is a proof of that CO_2 forms complex through electron donor−acceptor interactions.[67] Meanwhile, the new peak at 655 cm^{-1} in spectrum E is another distinct evidence of CO_2 forming complex according to literature.[67] After CO_2 has been desorbed from the hybrid membrane for 20 min (spectrum F), the peak at 655 cm^{-1} disappears and the peak at 2400−2300 cm^{-1} turns to be same shape as that in spectrum B, indicating that the reversible interaction disappears while only physical adsorption still exists in the membrane. After CO_2 has been desorbed from the hybrid membrane for 6 h (spectrum G), CO_2 peaks disappear and the spectrum looks similar to that of hybrid membrane without absorbing CO_2 (spectrum D), implying that all CO_2 is desorbed from the membrane. Thus, CO_2 could reversibly interact with the hybrid membrane but could not interact with the unfilled PI membrane, indicating that the interaction should be attributed to the addition of the SBMA@CNT particles. To be more specific, in these hybrid membranes, pSBMA layer with quaternary ammonium could conduct as facilitated transport channels at the interface between SBMA@CNT and polymer matrix. In these interconnected channels, CO_2 molecules rapidly pass through due to the reversible reaction with quaternary nitrogen, which results in significantly enhanced CO_2 permeability.

Second, CO_2 permeability is increased due to the improved water uptake of membrane. Both bound water and free water could significantly increase the CO_2 permeability while bound water could simultaneously maintain a preferable selectivity.[68,69] Before interpreting the hybrid membrane property, the unfilled PI membrane property at the dry state and humidified state should be compared first. The humidified PI membrane (after immersed in water for 10 days) shows a distinctly increased CO_2 permeability of 49.8 Barrer compared to 6.2 Barrer at the dry state, which is benefited from water swelling. On one hand, water could enhance polymer chain mobility, enlarge the space between polymer chains[70] and lead to increased gas permeability in polymer matrix. On the other hand, water itself could serve as a highly permeable region within the membrane because CO_2 permeability in pure water is as high as 1923 Barrer,[71] quite higher than those of most polymer matrices. For a hybrid membrane, when the SBMA@CNT content increases, the highly hydrophilic pSBMA forms a strongly bonded water layer, leads to an increased water uptake and further increases CO_2 permeability. CO_2 permeability shows a maximum when the particle content is 5 wt %, then turns to decease when the particle content becomes even higher. It might because the strong cohesion between excessively interconnected SBMA@CNT generates a much more confined space in the polymer network and limits gas transport and the water swelling degree, ultimately rendering lower CO_2 permeability.

In general, CO_2/CH_4 selectivity is positively correlated with the bound water portion in these membranes. The result corresponds to the beneficial effect of bound water on CO_2 transport. Quaternary ammonium of pSBMA selectively facilitates CO_2 transport with the assistance of the inner bound water layer. In the outer free water layer, CO_2 selectivity is relatively lower than that in the bound water layer, just as in

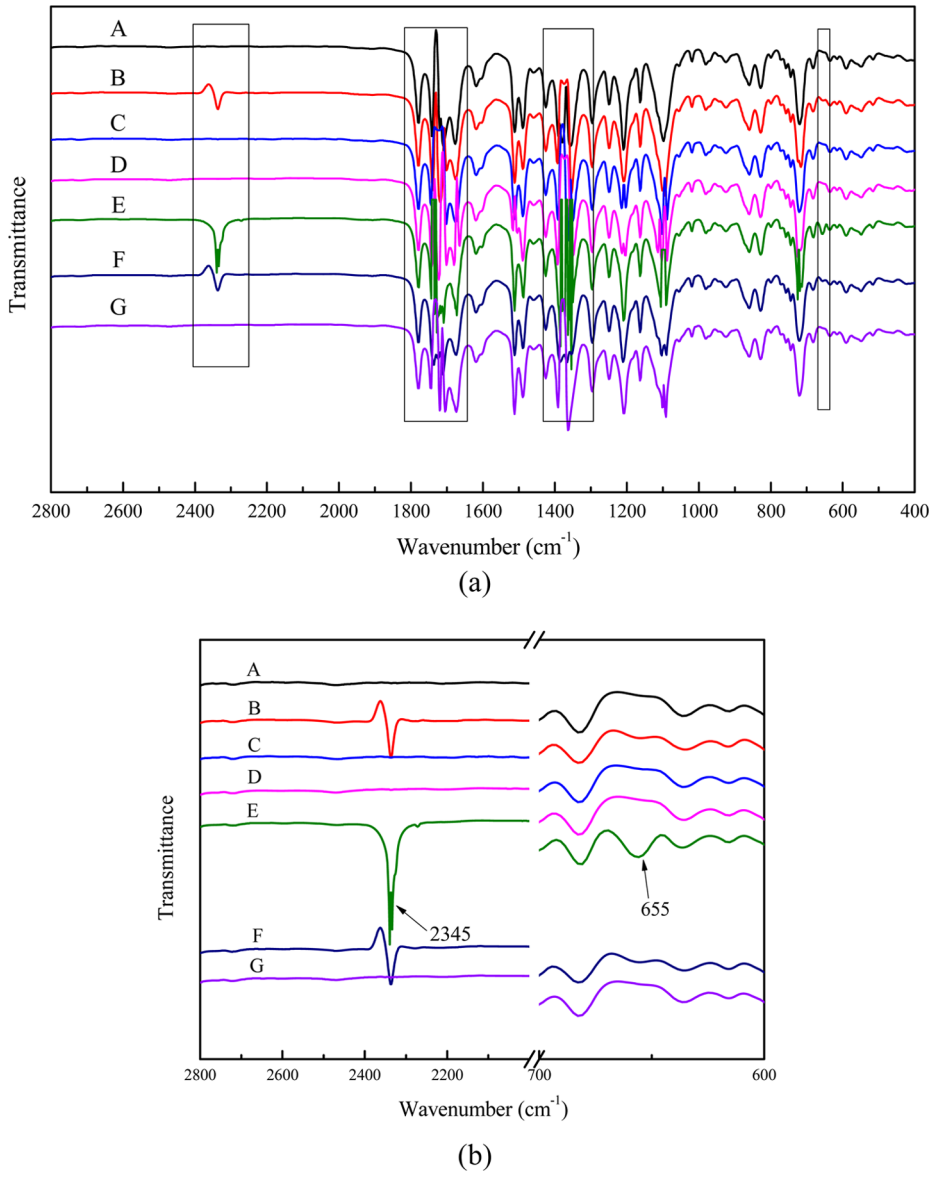

Figure 6. FTIR spectra of CO_2 adsorption and desorption within membranes. A, PI membrane; B, CO_2-absorbed PI membrane; C, CO_2-desorbed PI membrane; D, hybrid membrane; E, CO_2-absorbed hybrid membrane; F, CO_2-desorbed hybrid membrane (20 min); G, CO_2-desorbed hybrid membrane (6 h).

bulk water. In other words, excessive free water in the membrane would lead to lowered selectivity.[68,69] When the particle content is 5 wt %, the hybrid membrane possesses the highest total water uptake but the lowest bound water portion, which results in the highest CO_2 permeability but the lowest selectivity.

Because few previous studies simultaneously provide gas permeation test results at both dry and humidified states, the comparison of membrane performances between these two states in this study might provide an insight into the key effect of water.

3.4. Pressure Test. A pressure test is conducted at 2−16 bar to acquire more comprehensive information about membrane performance. As shown in Figure 7a, CO_2 permeability shows a minimum at about 8 bar, the so-called plasticization pressure. Meanwhile, CO_2/CH_4 selectivity monotonously decreases with the increased feed pressure. At pressures lower than 8 bar, CO_2 permeability decreases with the increased pressure due to the saturation of Langmuir absorption sites.[72] When the pressure is further raised to 16 bar, high CO_2 concentration swells the polymer matrix, disrupts the chain packing and enhances the chain mobility, resulting in increased CO_2 permeability. Meanwhile, CO_2 induced plasticization accelerates CH_4 transport because of the enhanced polymer chain mobility and enlarged free volume in membrane, resulting in decreased selectivity.[73,74] The plasticization pressure in this study is relatively low and it might be caused by the presence of water, which is also a plasticizer in a polymer matrix and leads to an accelerated plasticization. A lot of studies indicate that the plasticization phenomenon could be effectively suppressed by thermal annealing or cross-linking, whereas it is out of our concern in this study. The membranes in this study are not treated through thermal or chemical methods for antiplasticization and show typical CO_2 induced plasticization effect on polyimide membranes.

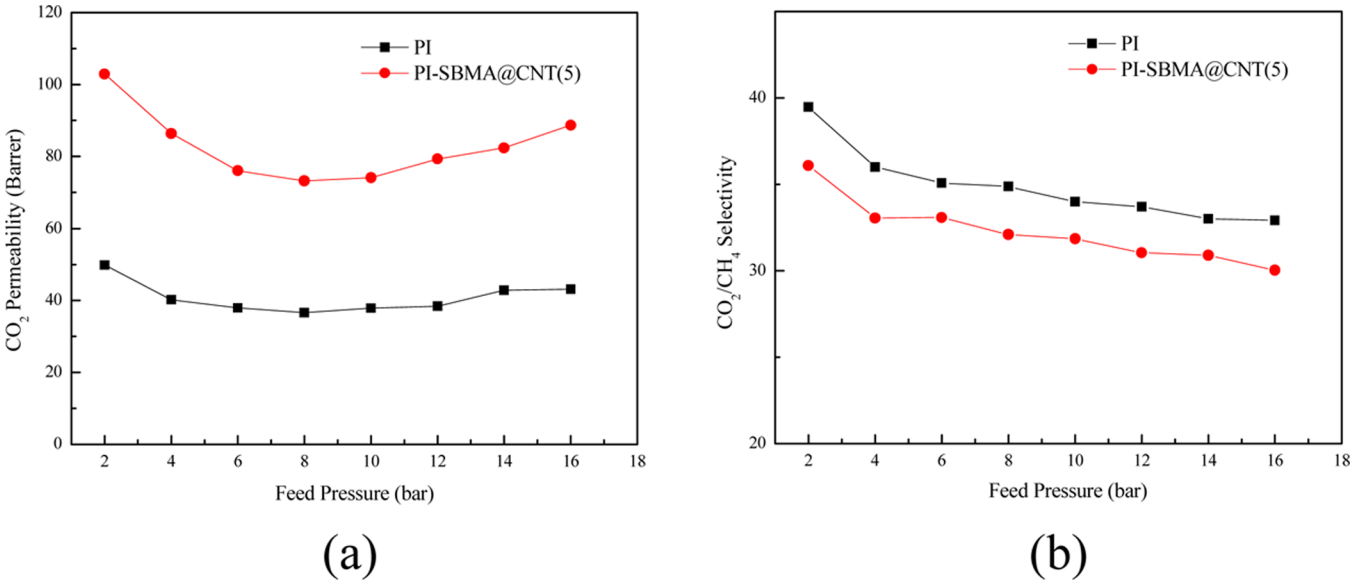

Figure 7. (a) Effect of feed pressure on CO_2 permeability of membrane and (b) effect of feed pressure on CO_2/CH_4 selectivity of membrane.

4. CONCLUSION

A novel hybrid membrane is designed and prepared by incorporating SBMA@CNT composite particles into a polyimide matrix. The hybrid membrane shows significantly increased CO_2 permeability compared to an unfilled PI membrane due to the existence of multifunctional polyzwitterion. When the particle content is 5 wt %, the hybrid membrane exhibits the maximum CO_2 permeability of 103 Barrer with CO_2/CH_4 selectivity of 36. The enhanced CO_2 separation property primarily arises from the facilitated transport effect of SBMA@CNT composite particles. Meanwhile, the particles also enhance the water uptake of the membrane, which further increases the CO_2 permeability. Selectivity of the membrane is dependent on the bound water portion in the membrane. The different separation performance of membranes at the humidified state and dry state indicates the crucial role of water.

The enhanced separation performance of the hybrid membrane suggests the potential application of a polyzwitterion material in modifying CO_2 capture membranes, especially those membranes with a rigid and hydrophobic polymer chain.

AUTHOR INFORMATION

Corresponding Author

*Z. Jiang. Fax: +86 22 2350 0086. Tel: +86 22 2350 0086. E-mail: zhyjiang@tju.edu.cn.

Notes

The authors declare no competing financial interest.

ACKNOWLEDGMENTS

We gratefully acknowledge the financial support from the National High Technology Research and Development Program of China (2012AA03A611), the National Science Fund for Distinguished Young Scholars (No. 21125627) and Program of Introducing Talents of Discipline to Universities (B06006).

REFERENCES

(1) D'Alessandro, D. M.; Smit, B.; Long, J. R. Carbon Dioxide Capture: Prospects for New Materials. *Angew. Chem., Int. Ed.* **2010**, *49*, 6058−6082.

(2) Jacobson, M. Z. Review of Solutions to Global Warming, Air Pollution, and Energy Security. *Energy Environ. Sci.* **2009**, *2*, 148−173.

(3) MacDowell, N.; Florin, N.; Buchard, A.; Hallett, J.; Galindo, A.; Jackson, G.; Adjiman, C. S.; Williams, C. K.; Shah, N.; Fennell, P. An Overview of CO_2 Capture Technologies. *Energy Environ. Sci.* **2010**, *3*, 1645−1669.

(4) Gin, D. L.; Noble, R. D. Designing the Next Generation of Chemical Separation Membranes. *Science* **2011**, *332*, 674−676.

(5) Xiao, Y.; Chung, T.-S. Grafting Thermally Labile Molecules on Cross-Linkable Polyimide to Design Membrane Materials for Natural Gas Purification and CO_2 Capture. *Energy Environ. Sci.* **2011**, *4*, 201−208.

(6) Staudt-Bickel, C.; J Koros, W. Improvement of CO_2/CH_4 Separation Characteristics of Polyimides by Chemical Crosslinking. *J. Membr. Sci.* **1999**, *155*, 145−154.

(7) Chung, T.-S.; Jiang, L. Y.; Li, Y.; Kulprathipanja, S. Mixed Matrix Membranes (MMMs) Comprising Organic Polymers with Dispersed Inorganic Fillers for Gas Separation. *Prog. Polym. Sci.* **2007**, *32*, 483−507.

(8) Powell, C. E.; Qiao, G. G. Polymeric CO_2/N_2 Gas Separation Membranes for the Capture of Carbon Dioxide from Power Plant Flue Gases. *J. Membr. Sci.* **2006**, *279*, 1−49.

(9) Rezakazemi, M.; Ebadi Amooghin, A.; Montazer-Rahmati, M. M.; Ismail, A. F.; Matsuura, T. State-of-the-Art Membrane based CO_2 Separation Using Mixed Matrix Membranes (MMMs): An Overview on Current Status and Future Directions. *Prog. Polym. Sci.* **2014**, *39*, 817−861.

(10) Wind, J. D.; Paul, D. R.; Koros, W. J. Natural Gas Permeation in Polyimide Membranes. *J. Membr. Sci.* **2004**, *228*, 227−236.

(11) Qiu, W.; Chen, C.-C.; Xu, L.; Cui, L.; Paul, D. R.; Koros, W. J. Sub-T_g Cross-Linking of a Polyimide Membrane for Enhanced CO_2 plasticization Resistance for Natural Gas Separation. *Macromolecules* **2011**, *44*, 6046−6056.

(12) Park, J.; Paul, D. Correlation and Prediction of Gas Permeability in Glassy Polymer Membrane Materials via a Modified Free Volume based Group Contribution Method. *J. Membr. Sci.* **1997**, *125*, 23−39.

(13) Horn, N. R.; Paul, D. R. Carbon Dioxide Plasticization and Conditioning Effects in Thick Vs. Thin Glassy Polymer Films. *Polymer* **2011**, *52*, 1619−1627.

(14) Kocherlakota, L. S.; Knorr, D. B.; Foster, L.; Overney, R. M. Enhanced Gas Transport Properties and Molecular Mobilities in Nano-Constrained Poly[1-(trimethylsilyl)-1-propyne] Membranes. *Polymer* **2012**, *53*, 2394−2401.

(15) Yampolskii, Y. Polymeric Gas Separation Membranes. *Macromolecules* **2012**, *45*, 3298−3311.
(16) Robeson, L. M. Correlation of Separation Factor Versus Permeability for Polymeric Membranes. *J. Membr. Sci.* **1991**, *62*, 165−185.
(17) Lau, C. H.; Li, P.; Li, F.; Chung, T.-S.; Paul, D. R. Reverse-Selective Polymeric Membranes for Gas Separations. *Prog. Polym. Sci.* **2013**, *38*, 740−766.
(18) Du, N.; Park, H. B.; Dal-Cin, M. M.; Guiver, M. D. Advances in High Permeability Polymeric Membrane Materials for CO_2 Separations. *Energy Environ. Sci.* **2012**, *5*, 7306−7322.
(19) Sanders, D. F.; Smith, Z. P.; Guo, R.; Robeson, L. M.; McGrath, J. E.; Paul, D. R.; Freeman, B. D. Energy-Efficient Polymeric Gas Separation Membranes for a Sustainable Future: A Review. *Polymer* **2013**, *54*, 4729−4761.
(20) Sridhar, S.; Veerapur, R. S.; Patil, M. B.; Gudasi, K. B.; Aminabhavi, T. M. Matrimid Polyimide Membranes for the Separation of Carbon Dioxide from Methane. *J. Appl. Polym. Sci.* **2007**, *106*, 1585−1594.
(21) Brunetti, A.; Scura, F.; Barbieri, G.; Drioli, E. Membrane Technologies for CO_2 Separation. *J. Membr. Sci.* **2010**, *359*, 115−125.
(22) Kim, T.; Koros, W.; Husk, G.; O'brien, K. Relationship between Gas Separation Properties and Chemical Structure in a Series of Aromatic Polyimides. *J. Membr. Sci.* **1988**, *37*, 45−62.
(23) Tanaka, K.; Kita, H.; Okano, M.; Okamoto, K.-i. Permeability and Permselectivity of Gases in Fluorinated and Non-Fluorinated Polyimides. *Polymer* **1992**, *33*, 585−592.
(24) Hayashi, J.-i.; Yamamoto, M.; Kusakabe, K.; Morooka, S. Simultaneous Improvement of Permeance and Permselectivity of 3,3′,4,4′-Biphenyltetracarboxylic Dianhydride-4,4′-oxydianiline Polyimide Membrane by Carbonization. *Ind. Eng. Chem. Res.* **1995**, *34*, 4364−4370.
(25) Lin, W. H.; Vora, R. H.; Chung, T. S. Gas Transport Properties of 6FDA-Durene/1,4-Phenylenediamine (PPDA) Copolyimides. *J. Polym. Sci., Part B: Polym. Phys.* **2000**, *38*, 2703−2713.
(26) Nagel, C.; Günther-Schade, K.; Fritsch, D.; Strunskus, T.; Faupel, F. Free Volume and Transport Properties in Highly Selective Polymer Membranes. *Macromolecules* **2002**, *35*, 2071−2077.
(27) Ghanem, B. S.; McKeown, N. B.; Budd, P. M.; Selbie, J. D.; Fritsch, D. High-Performance Membranes from Polyimides with Intrinsic Microporosity. *Adv. Mater.* **2008**, *20*, 2766−2771.
(28) Yong, H. H.; Park, H. C.; Kang, Y. S.; Won, J.; Kim, W. N. Zeolite-filled Polyimide Membrane Containing 2,4,6-Triaminopyrimidine. *J. Membr. Sci.* **2001**, *188*, 151−163.
(29) Cornelius, C. J.; Marand, E. Hybrid Silica-Polyimide Composite Membranes: Gas Transport Properties. *J. Membr. Sci.* **2002**, *202*, 97−118.
(30) Aroon, M. A.; Ismail, A. F.; Montazer-Rahmati, M. M.; Matsuura, T. Effect of Raw Multi-Wall Carbon Nanotubes on Morphology and Separation Properties of Polyimide Membranes. *Sep. Sci. Technol.* **2010**, *45*, 2287−2297.
(31) Aroon, M. A.; Ismail, A. F.; Montazer-Rahmati, M. M.; Matsuura, T. Effect of Chitosan as a Functionalization Agent on the Performance and Separation Properties of Polyimide/Multi-Walled Carbon Nanotubes Mixed Matrix Flat Sheet Membranes. *J. Membr. Sci.* **2010**, *364*, 309−317.
(32) Li, F.; Li, Y.; Chung, T.-S.; Kawi, S. Facilitated Transport by Hybrid Poss®−Matrimid®−Zn^{2+} Nanocomposite Membranes for the Separation of Natural Gas. *J. Membr. Sci.* **2010**, *356*, 14−21.
(33) Khan, A. L.; Klaysom, C.; Gahlaut, A.; Khan, A. U.; Vankelecom, I. F. J. Mixed Matrix Membranes Comprising of Matrimid and −So_3h Functionalized Mesoporous Mcm-41 for Gas Separation. *J. Membr. Sci.* **2013**, *447*, 73−79.
(34) Peydayesh, M.; Asarehpour, S.; Mohammadi, T.; Bakhtiari, O. Preparation and Characterization of SAPO-34−Matrimid® 5218 Mixed Matrix Membranes for CO_2/CH_4 Separation. *Chem. Eng. Res. Des.* **2013**, *91*, 1335−1342.
(35) Shindo, R.; Kishida, M.; Sawa, H.; Kidesaki, T.; Sato, S.; Kanehashi, S.; Nagai, K. Characterization and Gas Permeation Properties of Polyimide/ZSM-5 Zeolite Composite Membranes Containing Ionic Liquid. *J. Membr. Sci.* **2014**, *454*, 330−338.
(36) Li, Y.; He, G.; Wang, S.; Yu, S.; Pan, F.; Wu, H.; Jiang, Z. Recent Advances in the Fabrication of Advanced Composite Membranes. *J. Mater. Chem. A* **2013**, *1*, 10058−10077.
(37) Chen, G. Q.; Scholes, C. A.; Qiao, G. G.; Kentish, S. E. Water Vapor Permeation in Polyimide Membranes. *J. Membr. Sci.* **2011**, *379*, 479−487.
(38) Chen, G. Q.; Scholes, C. A.; Doherty, C. M.; Hill, A. J.; Qiao, G. G.; Kentish, S. E. Modeling of the Sorption and Transport Properties of Water Vapor in Polyimide Membranes. *J. Membr. Sci.* **2012**, *409−410*, 96−104.
(39) Scholes, C. A.; Tao, W. X.; Stevens, G. W.; Kentish, S. E. Sorption of Methane, Nitrogen, Carbon Dioxide, and Water in Matrimid 5218. *J. Appl. Polym. Sci.* **2010**, *117*, 2284−2289.
(40) Pourafshari Chenar, M.; Soltanieh, M.; Matsuura, T.; Tabe-Mohammadi, A.; Khulbe, K. C. The Effect of Water Vapor on the Performance of Commercial Polyphenylene Oxide and Cardo-Type Polyimide Hollow Fiber Membranes in CO_2/CH_4 Separation Applications. *J. Membr. Sci.* **2006**, *285*, 265−271.
(41) Reijerkerk, S. R.; Jordana, R.; Nijmeijer, K.; Wessling, M. Highly Hydrophilic, Rubbery Membranes for CO_2 Capture and Dehydration of Flue Gas. *Int. J. Greenhouse Gas Control* **2011**, *5*, 26−36.
(42) Chen, G. Q.; Scholes, C. A.; Doherty, C. M.; Hill, A. J.; Qiao, G. G.; Kentish, S. E. The Thickness Dependence of Matrimid Films in Water Vapor Permeation. *Chem. Eng. J.* **2012**, *209*, 301−312.
(43) Jiang, S.; Cao, Z. Ultralow-Fouling, Functionalizable, and Hydrolyzable Zwitterionic Materials and Their Derivatives for Biological Applications. *Adv. Mater.* **2010**, *22*, 920−932.
(44) Cheng, G.; Zhang, Z.; Chen, S.; Bryers, J. D.; Jiang, S. Inhibition of Bacterial Adhesion and Biofilm Formation on Zwitterionic Surfaces. *Biomaterials* **2007**, *28*, 4192−4199.
(45) Taki, K.; Hosokawa, K.; Takagi, S.; Mabuchi, H.; Ohshima, M. Rapid Production of Ultralow Dielectric Constant Porous Polyimide Films Via CO_2-tert-Amine Zwitterion-induced Phase Separation and Subsequent Photopolymerization. *Macromolecules* **2013**, *46*, 2275−2281.
(46) Chen, S.; Zheng, J.; Li, L.; Jiang, S. Strong Resistance of Phosphorylcholine Self-Assembled Monolayers to Protein Adsorption: Insights into Nonfouling Properties of Zwitterionic Materials. *J. Am. Chem. Soc.* **2005**, *127*, 14473−14478.
(47) Shao, Q.; He, Y.; White, A. D.; Jiang, S. Difference in Hydration between Carboxybetaine and Sulfobetaine. *J. Phys. Chem. B* **2010**, *114*, 16625−16631.
(48) Wu, J.; Lin, W.; Wang, Z.; Chen, S.; Chang, Y. Investigation of the Hydration of Nonfouling Material Poly(Sulfobetaine Methacrylate) by Low-Field Nuclear Magnetic Resonance. *Langmuir* **2012**, *28*, 7436−7441.
(49) Shishatskiy, S.; Pauls, J. R.; Nunes, S. P.; Peinemann, K.-V. Quaternary Ammonium Membrane Materials for CO_2 Separation. *J. Membr. Sci.* **2010**, *359*, 44−53.
(50) Blasig, A.; Tang, J.; Hu, X.; Tan, S. P.; Shen, Y.; Radosz, M. Carbon Dioxide Solubility in Polymerized Ionic Liquids Containing Ammonium and Imidazolium Cations from Magnetic Suspension Balance: P[VBTMA][BF_4] and P[VBMI][BF_4]. *Ind. Eng. Chem. Res.* **2007**, *46*, 5542−5547.
(51) Wang, J.; Yue, X.; Zhang, Z.; Yang, Z.; Li, Y.; Zhang, H.; Yang, X.; Wu, H.; Jiang, Z. Enhancement of Proton Conduction at Low Humidity by Incorporating Imidazole Microcapsules into Polymer Electrolyte Membranes. *Adv. Funct. Mater.* **2012**, *22*, 4539−4546.
(52) He, G.; Li, Z.; Li, Y.; Li, Z.; Wu, H.; Yang, X.; Jiang, Z. Zwitterionic Microcapsules as Water Reservoirs and Proton Carriers within a Nafion Membrane to Confer High Proton Conductivity under Low Humidity. *ACS Appl. Mater. Interfaces* **2014**, *6*, 5362−5366.
(53) El-Azzami, L. A.; Grulke, E. A. Parametric Study of CO_2 Fixed Carrier Facilitated Transport through Swollen Chitosan Membranes. *Ind. Eng. Chem. Res.* **2008**, *48*, 894−902.
(54) Li, Y.; Xin, Q.; Hong, W.; Guo, R.; Tian, Z.; Liu, Y.; Wang, S.; He, G.; Pan, F.; Jiang, Z. Efficient CO_2 Capture by Humidified

Polymer Electrolyte Membranes with Tunable Water State. *Energy Environ. Sci.* **2014**, *7*, 1489−1499.
(55) Francisco, G. J.; Chakma, A.; Feng, X. Membranes Comprising of Alkanolamines Incorporated into Poly(vinyl alcohol) Matrix for CO_2/N_2 Separation. *J. Membr. Sci.* **2007**, *303*, 54−63.
(56) Liu, L.; Chakma, A.; Feng, X. Gas Permeation through Water-Swollen Hydrogel Membranes. *J. Membr. Sci.* **2008**, *310*, 66−75.
(57) Car, A.; Stropnik, C.; Yave, W.; Peinemann, K.-V. PEG Modified Poly(amide-b-ethylene oxide) Membranes for CO_2 Separation. *J. Membr. Sci.* **2008**, *307*, 88−95.
(58) Kasák, P.; Kroneková, Z.; Krupa, I.; Lacík, I. Zwitterionic Hydrogels Crosslinked with Novel Zwitterionic Crosslinkers: Synthesis and Characterization. *Polymer* **2011**, *52*, 3011−3020.
(59) Inagaki, M.; Ohta, N.; Hishiyama, Y. Aromatic Polyimides as Carbon Precursors. *Carbon* **2013**, *61*, 1−21.
(60) Quinn, F. X.; Kampff, E.; Smyth, G.; McBrierty, V. J. Water in Hydrogels. 1. A Study of Water in Poly(*N*-vinyl-2-pyrrolidone/methyl methacrylate) Copolymer. *Macromolecules* **1988**, *21*, 3191−3198.
(61) Qu, X.; Wirsen, A.; Albertsson, A.-C. Novel pH-Sensitive Chitosan Hydrogels: Swelling Behavior and States of Water. *Polymer* **2000**, *41*, 4589−4598.
(62) Choi, J.-H.; Jegal, J.; Kim, W. N. Modification of Performances of Various Membranes Using MWNTs as a Modifier. *Macromol. Symp.* **2007**, *249*−*250*, 610−617.
(63) Peng, F.; Hu, C.; Jiang, Z. Novel Ploy(vinyl alcohol)/Carbon Nanotube Hybrid Membranes for Pervaporation Separation of Benzene/Cyclohexane Mixtures. *J. Membr. Sci.* **2007**, *297*, 236−242.
(64) Deng, J.; Zhang, X.; Wang, K.; Zou, H.; Zhang, Q.; Fu, Q. Synthesis and Properties of Poly(ether urethane) Membranes Filled with Isophorone Diisocyanate-Grafted Carbon Nanotubes. *J. Membr. Sci.* **2007**, *288*, 261−267.
(65) Wang, M.; Wang, Z.; Wang, J.; Zhu, Y.; Wang, S. An Antioxidative Composite Membrane with the Carboxylate Group as a Fixed Carrier for CO_2 Separation from Flue Gas. *Energy Environ. Sci.* **2011**, *4*, 3955.
(66) Wang, Z.; Li, M.; Cai, Y.; Wang, J.; Wang, S. Novel CO_2 Selectively Permeating Membranes Containing PETEDA Dendrimer. *J. Membr. Sci.* **2007**, *290*, 250−258.
(67) Meredith, J. C.; Johnston, K. P.; Seminario, J. M.; Kazarian, S. G.; Eckert, C. A. Quantitative Equilibrium Constants between CO_2 and Lewis Bases from FTIR Spectroscopy. *J. Phys. Chem.* **1996**, *100*, 10837−10848.
(68) El-Azzami, L. A.; Grulke, E. A. Carbon Dioxide Separation from Hydrogen and Nitrogen by Fixed Facilitated Transport in Swollen Chitosan Membranes. *J. Membr. Sci.* **2008**, *323*, 225−234.
(69) El-Azzami, L. A.; Grulke, E. A. Carbon Dioxide Separation from Hydrogen and Nitrogen Facilitated Transport in Arginine Salt−Chitosan Membranes. *J. Membr. Sci.* **2009**, *328*, 15−22.
(70) Hodge, R.; Bastow, T.; Edward, G.; Simon, G.; Hill, A. Free Volume and the Mechanism of Plasticization in Water-Swollen Poly(vinyl alcohol). *Macromolecules* **1996**, *29*, 8137−8143.
(71) Liu, L.; Chakma, A.; Feng, X. Gas Permeation through Water-Swollen Hydrogel Membranes. *J. Membr. Sci.* **2008**, *310*, 66−75.
(72) Chua, M. L.; Xiao, Y. C.; Chung, T.-S. Modifying the Molecular Structure and Gas Separation Performance of Thermally Labile Polyimide-based Membranes for Enhanced Natural Gas Purification. *Chem. Eng. Sci.* **2013**, *104*, 1056−1064.
(73) Bos, A.; Pünt, I.; Wessling, M.; Strathmann, H. Plasticization-Resistant Glassy Polyimide Membranes for CO_2/CH_4 Separations. *Sep. Purif. Technol.* **1998**, *14*, 27−39.
(74) Thundyil, M. J.; Jois, Y. H.; Koros, W. J. Effect of Permeate Pressure on the Mixed Gas Permeation of Carbon Dioxide and Methane in a Glassy Polyimide. *J. Membr. Sci.* **1999**, *152*, 29−40.